

Field Theory Design of Square Waveguide Iris Polarizers

ULRICH TUCHOLKE, FRITZ ARNDT, SENIOR MEMBER, IEEE, AND THOMAS WRIEDT

Abstract—Profiled depth corrugated square waveguide polarizers are designed with the method of field expansion into eigenmodes, which includes higher order mode interaction between the step discontinuities. Computer-optimized design data are given for a compact Ku-band prototype with an exponentially varying depth function that achieves $90^\circ \pm 1^\circ$ differential phase shift within the separate 11.9–12.3-GHz and 17.5–17.9-GHz frequency bands. The maximum VSWR is only about 1.02. Further design examples include a linearly profiled depth function, which provides a short design, and a polarizer with iris thicknesses suitable for metal-etching manufacturing technique. The theory is verified by comparison with available measured results.

I. INTRODUCTION

E-PLANE CORRUGATED rectangular waveguide polarizers [1]–[5] have found widespread application for exciting circularly polarized waves in square-aperture antennas. In the previous designs [1]–[5], the differential 90° phase shift required between the orthogonal TE_{10} and TE_{01} mode is produced by periodic corrugation. Although ramp sections are usually employed at the input and output ports, due to the periodic loading principle of this kind of polarizers, difficulties may often arise to insure good broad-band impedance match.

Since there is increasing demand for polarizers capable of maintaining their properties over wide bandwidths, or at widely separated specific bands (such as the satellite bands), in this paper a profiled depth corrugated polarizer is suggested (Fig. 1) that may help to alleviate the broad-band matching problem. Moreover, by utilizing an appropriate profile function that yields suitable slot depth together with sufficient broad-band match, the number of corrugations may be reduced with regard to a comparable periodically corrugated design.

Opposite to the well-established theories based on a lumped loading concept [1], on an anisotropic surface impedance of the corrugated geometry [2], [3], [6], [7], or on cavity eigenfunctions [5], [15], an accurate field theory method for computer-aided design is used [4], [8], [14]. This allows direct inclusion of higher order mode coupling effects as well as satisfying all actual boundary conditions exactly. Matching the field at common interfaces yields the scattering matrix of the corresponding discontinuity. As for the overall scattering matrix, the used direct combination of the involved individual scattering matrices at all

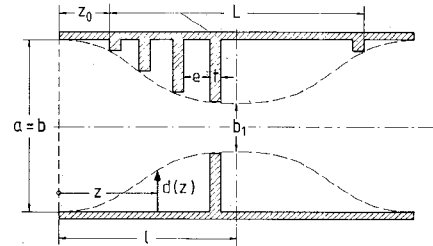


Fig. 1. Profiled depth corrugated square waveguide polarizer.

step discontinuities [8] avoids numerical instabilities by the otherwise known situation of interacting discontinuities. Therefore, no further improvement of the analysis is necessary, e.g., by termination of modes by their characteristic admittances [9], [10]. Besides the numerical stability, a further advantage of this direct calculation, in comparison with the common transmission matrix method, is that no symmetry of ports (i.e., modes) is required. Therefore, there is no need to maintain the number of “localized” [9] modes, necessary for calculating the scattering matrix of the irises, for the “accessible” [9] modes within a homogeneous waveguide section between them. This helps to reduce the computing time and storage requirements.

An optimizing computer program varies the polarizer parameters until differential phase shift and input VSWR, both for TE_{10} and TE_{01} incidence, correspond to predicted amounts. The evolution strategy method [11]—a modified direct search method [17]—where the parameters of the error function are varied statistically, is utilized. The standard deviation σ of the pseudo-normal distribution is controlled by a strategy parameter H , which is successively diminished after each successful iteration step; H is multiplied by a factor $10^3, \dots, 10^5$, if the error function shows an asymptotic behavior. The advantages are such that local minima may be avoided and no differentiation step in the calculation algorithm is necessary.

In addition to the profiled depth corrugated polarizer (Fig. 1) that provides the best VSWR behavior combined with a compact size, two further polarizer types of possibly practical importance are included in the design examples. A periodically corrugated type with iris thickness of $t = 190 \mu\text{m}$ in order to allow an accurate metal-etching manufacturing technique, and a polarizer with linearly tapered corrugation over the whole length which enables a short design. The comparison with available experimental and theoretical results [2], [3], [5], establishes the accuracy of the given theory by excellent agreement.

Manuscript received April 25, 1985; revised August 15, 1985.

The authors are with the Microwave Department, University of Bremen, Kufsteiner Str., NW1, D-2800 Bremen 33, West Germany.
IEEE Log Number 8405921.

II. THEORY

The exciting field at the input port of the square waveguide polarizer is considered to consist of the two fundamental TE_{10} and TE_{01} modes simultaneously. Therefore, the complete direct field solution of [8] can be used. Since the derivation of the scattering matrix of the polarizer structure is analogous to that one of the waveguide step transformer, [8], [14], the theory is given here in abbreviated form only. For details, the reader is referred to [8] and [14].

At the step discontinuities to be investigated, the field components are derived from the axial z -components of the magnetic and electric Hertzian vector potentials $\vec{\Pi}_h$ and $\vec{\Pi}_e$ [12]

$$\begin{aligned}\vec{E} &= -j\omega\mu\nabla \times \vec{\Pi}_{hz} + \nabla \times \nabla \times \vec{\Pi}_{ez} \\ \vec{H} &= j\omega\epsilon\nabla \times \vec{\Pi}_{ez} + \nabla \times \nabla \times \vec{\Pi}_{hz}.\end{aligned}\quad (1)$$

The vector potentials in (1) are assumed to be sums of eigenmodes satisfying the vector Helmholtz equation and the boundary condition at the metallic surfaces [13]

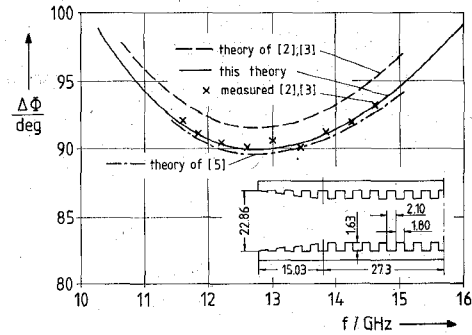
$$\begin{aligned}\Pi_{hz} &= \sum_{m=0}^M \sum_{n=0}^N A_{hmn} T_{hmn} + B_{hmn} T_{hmn} \\ \Pi_{ez} &= \sum_{m=1}^M \sum_{n=1}^N A_{emn} T_{emn} + B_{emn} T_{emn}\end{aligned}\quad (2)$$

with the eigenfunctions T normalized so [8] that the power carried by a given wave is proportional to the square of the mode coefficient A , B . For simplicity, the eigenmodes in (2) are written at $z=0$ only; the z -dependence in forward and backward direction is understood. $A_{h,e}$ and $B_{h,e}$ are the still unknown complex amplitude coefficients of the corresponding mode m , n . The types of modes used for expansion purposes for this kind of discontinuities problem are: $TE_{1n'}$, $TM_{1n''}$, or $TE_{1n'}$ (with $n' = 0, 2, 4, \dots, n'' = 2, 4, 6, \dots$), and $TE_{0n'''}$ (with $n''' = 1, 3, 5, \dots$). The number of modes necessary for calculating the scattering matrix of the irises depends on their thickness t . Utilizing the asymptotic behavior of the scattering parameters as a relative criterion, and the corresponding equivalent circuit parameters [18] as an absolute one, the most critical iris, with $t = 190\mu\text{m}$, requires "localized" [9] modes to be considered up to TE_{140} , TM_{140} (i.e., TE_{140}), and TE_{041} , respectively. As for the "accessible" [9] modes between the irises, only the first seven need to be considered, for this case. The "accessible" modes include all propagating modes and the first few evanescent modes, depending upon the distance between adjacent discontinuities [9].

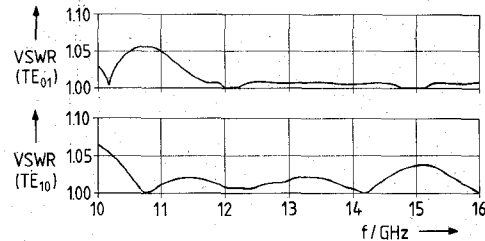
By matching the tangential field components at the corresponding interfaces of the step discontinuity considered, and utilizing the orthogonal properties of the eigenmodes [12], the coefficients $A_{h,e}$ and $B_{h,e}$ in (2) can be related to each other by the scattering matrix

$$(B) = (S) (A) \quad (3)$$

where (S) is given in [8], together with the corresponding



(a)



(b)

Fig. 2. Periodically corrugated polarizer. Data according to [2] and [3] (all dimensions in millimeters). (a) Differential phase shift $\Delta\phi = \arcsin(S_{21TE01}) - \arcsin(S_{21TE10})$ as a function of frequency. (b) VSWR for TE_{01} and TE_{10} incidence, respectively, as a function of frequency.

submatrices explained in [14]. The series of steps is calculated by direct combination of the single scattering matrices [8].

For the computer optimization of the polarizer an error function is defined

$$F(\bar{x}) = \sum_{i=1}^J (90^\circ - \Delta\phi(f_i))^2 + \sum_{i=1}^J |S_{11TE10}(f_i)|^2 + \sum_{i=1}^J |S_{11TE01}(f_i)|^2 \stackrel{!}{=} \min \quad (4)$$

where the E -plane corrugation and waveguide housing dimensions \bar{x} are optimized to yield a minimum, for a given number of corrugations and desired frequency range(s). In (4), $\Delta\phi$ is the differential phase shift calculated at the frequency sample points f_i , where a number of $J=10$ for one $90^\circ \pm 1^\circ$ frequency band (cf., Fig. 3(b)), or only $J=2$ for each of the two $90^\circ \pm 1^\circ$ frequency bands (cf., e.g., Fig. 3(c)), respectively, has turned out to be sufficient. Values S_{11TE10} and S_{11TE01} are the input reflection coefficients of the TE_{10} and TE_{01} wave, respectively.

III. RESULTS

Fig. 2(a) shows the differential phase shift $\Delta\phi = \arcsin(S_{21TE01}) - \arcsin(S_{21TE10})$ as a function of frequency for a periodically corrugated polarizer (22 irises) with design data given in [2], [3]. The phase shift curve calculated with this method (solid line) shows good agreement with the measured results of [2] and [3] and with the calculations of [5]. The linearly tapered ramp sections at the input and output ports of the original polarizer in [2] and [3] have been approximated by a corresponding staircase ramp. The

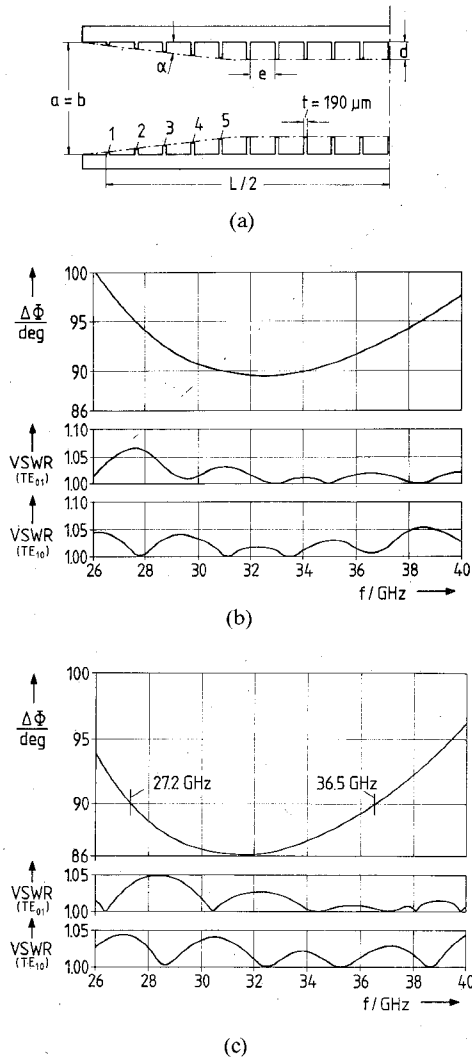


Fig. 3. Optimized *Ka*-band polarizer with 21 irises, periodic corrugation and ramp section, and a prescribed iris thickness of $t=190 \mu\text{m}$ for metal-etching manufacturing techniques. (a) Geometry, five ramp irises. Differential phase shift $\Delta\phi$, VSWR for TE_{01} , and TE_{10} incidence, respectively, as a function of frequency for. (b) One $90^\circ \pm 1^\circ$ frequency band; optimized polarizer dimensions: $a = b = 7.85 \text{ mm}$, $e = 1.552 \text{ mm}$, $d = 0.593 \text{ mm}$, $d_1 = 0.272 \text{ mm}$, $d_2 = 0.339 \text{ mm}$, $d_3 = 0.407 \text{ mm}$, $d_4 = 0.474 \text{ mm}$, $d_5 = 0.542 \text{ mm}$, $L = 35.03 \text{ mm}$. (c) Two $90^\circ \pm 1^\circ$ frequency bands, optimized polarizer dimensions: $a = b = 8.997 \text{ mm}$, $e = 1.403 \text{ mm}$, $d = 0.622 \text{ mm}$, $d_1 = 0.283 \text{ mm}$, $d_2 = 0.351 \text{ mm}$, $d_3 = 0.420 \text{ mm}$, $d_4 = 0.489 \text{ mm}$, $d_5 = 0.558 \text{ mm}$, $L = 32.05 \text{ mm}$.

calculated input VSWR, both for TE_{01} and TE_{10} incidence, is shown in Fig. 2(b).

The optimized *Ka*-band polarizer of Fig. 3(a) with 21 irises has a fixed iris thickness of $t=190 \mu\text{m}$, which allows an accurate metal-etching manufacturing technique [16]; metal sheets of $t=190 \mu\text{m}$ are commercially available.

For a prescribed number of irises, also in the ramp section (in this case: five irises), the optimization parameters \bar{x} in (4) are: waveguide width and height $a = b$, corrugation depth d , iris distance e , and the slope angle α of the corrugation depth in the ramp section. The differential phase shift $\Delta\phi$ shows a $\pm 1^\circ$ phase deviation, with regard to the desired 90° , between 30–34.5 GHz (design example Fig. 3(b)), as well as between 27–27.8 GHz, and 35.9–37.2 GHz (design example Fig. 3(c)), respectively. The linearly tapered matching ramp (five irises) provides a

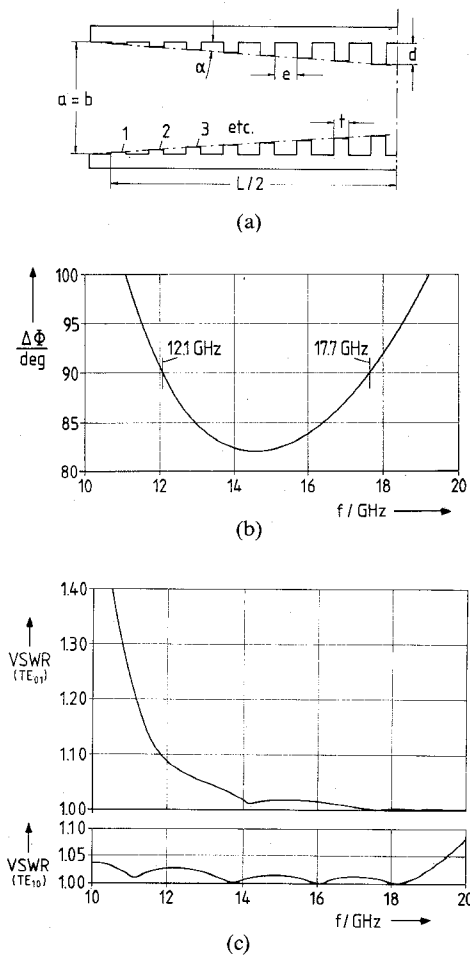


Fig. 4. Optimized *Ku*-band polarizer with 16 irises, and linearly tapered corrugation over the whole length. (a) Geometry. (b) Differential phase shift $\Delta\phi$ as a function of frequency. (c) VSWR for TE_{01} and TE_{10} incidence, respectively, as a function of frequency. Optimized polarizer dimensions: $a = b = 17.997 \text{ mm}$, $t = 0.942 \text{ mm}$, $e = 3.72 \text{ mm}$, $d = d_8 = 1.914 \text{ mm}$, $d_1 = 0.279 \text{ mm}$, $d_2 = 0.513 \text{ mm}$, $d_3 = 0.746 \text{ mm}$, $d_4 = 0.980 \text{ mm}$, $d_5 = 1.214 \text{ mm}$, $d_6 = 1.447 \text{ mm}$, $d_7 = 1.681 \text{ mm}$, $L = 70.86 \text{ mm}$.

maximum VSWR of 1.03 (Fig. 3(b)), and 1.05 (Fig. 3(c)), respectively, within the designed frequency band(s).

An optimized *Ku*-band polarizer with linearly tapered corrugation over the whole polarizer length, and 16 irises, Fig. 4(a)–(c), achieves a short design ($L = 70.86 \text{ mm}$). The optimization parameters \bar{x} in (4) are the waveguide dimensions $a = b$, the iris thickness t and distance e , as well as the linearly tapered corrugation profile function which is given by, e.g., the depth d and the angle α . Within the frequency bands of $90^\circ \pm 1^\circ$ differential phase shift, 12.0–12.2 GHz, and 17.5–18.0 GHz, respectively, the maximum VSWR is about 1.08.

The computer-aided design which provides the best VSWR behavior combined with a compact size, is the profiled depth corrugated polarizer (Figs. 1 and 5). An exponentially varying depth function to be optimized was chosen

$$d(z) = \frac{b}{2} \left\{ 1 - \exp \left[\ln \left(\frac{b_1}{b} \right) \left(\frac{z}{l} - \sin \left(2\pi \frac{z}{l} \right) \right) \right] \right\}. \quad (5)$$

For a given number of irises, the optimization parameters \bar{x} are: the waveguide housing dimensions $b = a$, the

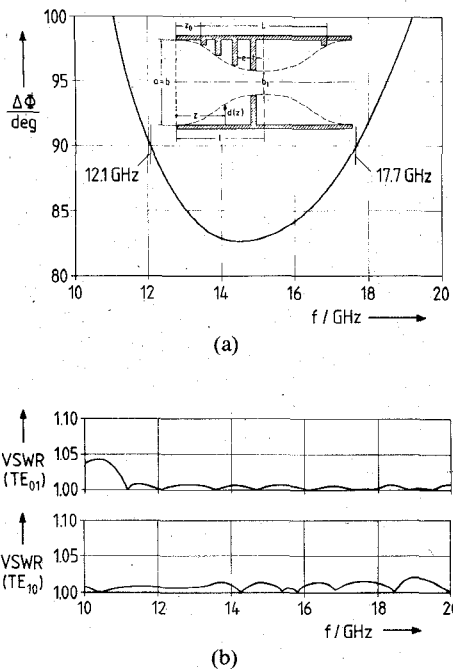


Fig. 5. Optimized profiled depth corrugated polarizer (Ku -band, 16 irises). (a) Differential phase shift $\Delta\phi$ as a function of frequency. (b) VSWR for TE_{01} and TE_{10} incidence, respectively, as a function of frequency. Optimized polarizer dimensions: $a = b = 18.377$ mm, $t = 1.295$ mm, $e = 4.171$ mm, depths of the corrugation (from left): $d_1 = 0.279$ mm, $d_2 = 0.521$ mm, $d_3 = 0.803$ mm, $d_4 = 1.080$ mm, $d_5 = 1.310$ mm, $d_6 = 1.470$ mm, $d_7 = 1.555$ mm, $d_8 = 1.582$ mm, $L = 83.27$ mm.

iris thickness t , the iris distance e , the minimum height b_1 of the iris aperture (cf. Fig. 1), and the place z_0 of the first iris.

In (5), the length l is given by $z_0 + L/2$, where L is the sum of all iris thicknesses and distances. Hence, the polarizer length L is implicitly included as an optimization parameter. Within the frequency bands of $90^\circ \pm 1^\circ$ differential phase shift, 11.9–12.3 GHz, and 17.5–17.9 GHz, respectively, the maximum VSWR of a 16 iris prototype (Figs. 5(a)–(b)) is only about 1.02. The overall length of the polarizer is 83.27 mm.

IV. CONCLUSION

A computer-aided design of profiled depth corrugated square waveguide polarizers is described, which enables the inclusion of higher order mode coupling effects and the exact field matching at all discontinuities. Application of the evolution strategy method leads to optimum low input VSWR, both for TE_{01} and TE_{10} incidence, respectively. The desired $90^\circ \pm 1^\circ$ differential phase shift may be achieved at widely separated specific bands, such as the satellite bands. In addition to the exponentially profiled depth corrugated polarizer, which provides the best VSWR behavior (maximum 1.02) combined with a compact size, the two further polarizer types shown may also be of practical importance: a periodically corrugated type with iris thickness of $t = 190 \mu\text{m}$ suitable for a metal-etching manufacturing technique, and a linearly profiled depth corrugated type which enables a short design. The comparison with available measured and theoretical results establishes the accuracy of the theory given.

ACKNOWLEDGMENT

The authors thank Dr. Fasold, Head of the Antenna Department of MBB, for financial support and for helpful discussions.

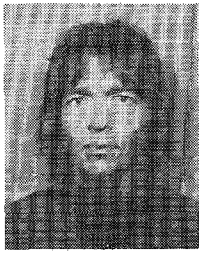
REFERENCES

- [1] A. J. Simmons, "Phase shift by periodic loading of waveguide and its applications to broad-band circular polarization," *IRE Trans. Microwave Theory Tech.*, vol. MTT-3, pp. 18–21, Dec. 1955.
- [2] N. Adatia, K. Keen, B. K. Watson, C. Crone, and N. Dang, "Study of an antenna system for an experimental TV satellite," ESA Contract Rep. 3285/77/NL/AK(SC), ERA Rep. RFTC 420877, Mar. 1979.
- [3] R. J. Dewey, "Circularly polarized elliptical beamshape horn antennas," *Int. J. Electron.*, vol. 53, no. 2, pp. 101–128, 1982.
- [4] F. Arndt, U. Tucholke, and T. Wriedt, "Broadband dual-depth E -plane corrugated square waveguide polariser," *Electron. Lett.*, vol. 20, no. 11, pp. 458–459, May 1984.
- [5] E. Kühn and B. K. Watson, "Rectangular corrugated horns-analysis, design and evaluation," in *Proc. 14th Euro. Microwave Conf.* (Liège), Sept. 1984.
- [6] A. M. B. Al-Hariri, A. D. Olver, and P. J. B. Clarricoats, "Low-attenuation properties of corrugated rectangular waveguide," *Electron. Lett.*, vol. 10, pp. 304–305, 1974.
- [7] G. H. Bryant, "Propagation in corrugated waveguides," *Proc. Inst. Elec. Eng.*, vol. 116, pp. 203–213, Feb. 1969.
- [8] H. Patzelt and F. Arndt, "Double-plane steps in rectangular waveguides and their applications for transformers, irises, and filters," *IEEE Trans. Microwave Theory Tech.*, vol. MTT-30, pp. 771–776, May 1982.
- [9] M. S. Navarro, T. T. Rozzi, and Y. T. Lo, "Propagation in a rectangular waveguide periodically loaded with resonant irises," *IEEE Trans. Microwave Theory Tech.*, vol. MTT-28, pp. 857–865, Aug. 1980.
- [10] T. Rozzi, "A new approach to the network modeling of capacitive irises and steps in waveguide," *Int. J. Circuit Theory Appl.*, vol. 3, pp. 339–354, Dec. 1975.
- [11] H. Schmiedel, "Anwendung der Evolutionsoptimierung bei Mikrowellenschaltungen," *Frequenz*, vol. 35, pp. 306–310, Nov. 1980.
- [12] R. E. Collin, *Field Theory of Guided Waves*. New York: McGraw-Hill, 1960, pp. 22–27, 174–179.
- [13] R. F. Harrington, *Time Harmonic Electromagnetic Fields*. New York: McGraw-Hill, 1961, pp. 171–177.
- [14] F. Arndt, U. Tucholke, and T. Wriedt, "Computer-optimized multi-section transformers between rectangular waveguides of adjacent frequency bands," *IEEE Trans. Microwave Theory Tech.*, vol. MTT-32, pp. 1479–1484, Nov. 1984.
- [15] K. Kurokawa, "The expansion of electromagnetic fields in cavities," *IRE Trans. Microwave Theory Tech.*, vol. MTT-6, pp. 178–187, Feb. 1958.
- [16] F. Arndt, B. Koch, H.-J. Orlok, and N. Schroeder, "Field theory design of rectangular waveguide broadwall metal-insert slot couplers for millimeter wave applications," *IEEE Trans. Microwave Theory Tech.*, vol. MTT-33, pp. 95–104, Feb. 1985.
- [17] R. Hooke and T. A. Jeves, "'Direct search' solution of numerical and statistical problems," *J. Assoc. Comp. Machinery*, vol. 8, pp. 212–229, 1961.
- [18] N. Marcuvitz, *Waveguide Handbook*. New York: McGraw-Hill, 1951, ch. 5.1.

✱



Ulrich Tucholke was born in Klein-Schlingen, West Germany, on June 20, 1956. In 1979, he received the Dipl.-Ing. (FH) from the Hochschule für Technik Bremen, Germany, where his major studies were on digital processing. He then joined the University of Bremen where he received the Dipl.-Ing. degree in 1983 for research in microwave applications (irises and transformers). Since then he has been with Prof. F. Arndt at the Microwave Department of the University of Bremen. He is presently working as a scientific assistant, concentrating on microwave filters and polarizers.



Fritz Arndt (SM'83) was born in Konstanz, Germany, on April 30, 1938. He received the Dipl.-Ing., the Dr.-Ing., and the Habilitation degrees from the Technical University of Darmstadt, Germany, in 1963, 1968, and 1972, respectively.

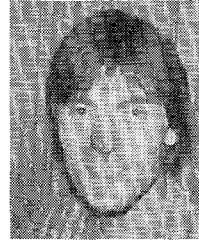
From 1963 to 1972, he worked on directional couplers and microstrip techniques at the Technical University of Darmstadt. Since 1972, he has been a Professor and Head of the Microwave Department at the University of Bremen,

Germany. His research activities are at present in the area of the solution of field problems of waveguide, finline, and optical waveguide structures, of antenna design, and of scattering structures.

Dr. Arndt is member of the VDE and NTG (Germany). He received the NTG award in 1970, the A.F. Bulgin Award (together with three

coauthors), in 1982 from the Institution of Radio and Electronic Engineers.

✱



Thomas Wriedt was born in Preetz, West Germany, on June 20, 1954. He received his Ing. grad. degree from the Fachhochschule Kiel, West Germany, in 1979 and his Dipl. Ing. degree from the University of Bremen, West Germany, in 1984.

Since 1984, he has been working as a Research Assistant on microwave components and antennas at the University of Bremen.